

Self-assembly of colloidal particles into strings in a homogeneous external electric or magnetic field

This article has been downloaded from IOPscience. Please scroll down to see the full text article.

2012 J. Phys.: Condens. Matter 24 464113

(<http://iopscience.iop.org/0953-8984/24/46/464113>)

View [the table of contents for this issue](#), or go to the [journal homepage](#) for more

Download details:

IP Address: 129.241.220.207

The article was downloaded on 16/08/2013 at 04:23

Please note that [terms and conditions apply](#).

Self-assembly of colloidal particles into strings in a homogeneous external electric or magnetic field

Frank Smallenburg, Hanumantha Rao Vutukuri, Arnout Imhof,
Alfons van Blaaderen and Marjolein Dijkstra

Soft Condensed Matter, Debye Institute for NanoMaterials Science, Utrecht University,
3584 CC Utrecht, The Netherlands

E-mail: f.smallenburg@gmail.com

Received 12 May 2012, in final form 25 June 2012

Published 31 October 2012

Online at stacks.iop.org/JPhysCM/24/464113

Abstract

Colloidal particles with a dielectric constant (magnetic susceptibility) mismatch with the surrounding solvent acquire a dipole moment in a homogeneous external electric (magnetic) field. The resulting dipolar interactions can lead to aggregation of the particles into string-like clusters. Recently, several methods have been developed to make these structures permanent. However, especially when multiple particle sizes and/or more complex shapes than single spheres are used, the parameter space for these experiments is enormous. We therefore use Monte Carlo simulations to investigate the structure of the self-assembled string-like aggregates in binary mixtures of dipolar hard and charged spheres, as well as dipolar hard asymmetric dumbbells. Binary mixtures of spheres aggregate in different types of clusters depending on the size ratio of the spheres. For highly asymmetric systems, the small spheres form ring-like and flame-like clusters around strings of large spheres, while for size ratios closer to 1, alternating strings of both large and small spheres are observed. For asymmetric dumbbells, we investigate both the effect of size ratio and dipole moment ratio, leading to a large variety of cluster shapes, including chiral clusters.

(Some figures may appear in colour only in the online journal)

1. Introduction

External electric or magnetic fields provide a powerful tool to control the self-assembly of colloidal particles. When an external field is applied to a colloidal suspension, the particles obtain a dipole moment as a result of the contrast of the dielectric constant or magnetic susceptibility of the particles with that of the fluid. At low field strengths, the resulting dipolar interactions between the colloids cause the particles to self-assemble into string-like structures along the field direction. These suspensions are called electro- (ER) or magneto- (MR) rheological fluids, as their rheological properties can be tuned dramatically by external fields on millisecond timescales [1, 2]. These fluids can be used in a wide range of applications, e.g. hydraulic valves, brakes, clutches [1] and displays [3]. For systems of monodisperse hard spheres with induced dipolar interactions,

the phase diagram is well known from both experiments and simulations [4–8]. A stable string fluid exists at low field strengths and at low packing fractions, while at higher field strengths, a body-centered-tetragonal (bct) crystal structure is formed.

Independently from each other, several groups have recently devised (physical) chemical methodologies to make strings of particles [9–16]. Our group recently developed a methodology to produce permanent strings of various colloidal particles by using external electric fields and a double layer repulsion comparable to the particle size followed by a thermal heating step or seeded growth to make the strings permanent [17]. This method allows control of both the length and even the flexibility of the chains of beads, making these systems interesting not only for making new materials but also as colloidal analogues of charged and uncharged polymer chains.

These electric string fluids can be compared to the formation of chain-like aggregates in ferromagnetic fluids, where the direction of the dipole moment of the particles is not fixed by an external field. The structure of these chains has been studied extensively, both for monodisperse and polydisperse systems [18–22]. In bidisperse or polydisperse systems, where the dipole moment scales with the particle volume, the larger particles dominate the formation of chains. Subsequently, the smaller particles can aggregate around these large-sphere structures, thereby hindering the formation of longer chains [23]. Previous studies showed that size polydispersity greatly influences the electrorheological response, which can even be enhanced in equimolar mixtures of large and small spheres [24]. Additionally, mixtures of particles with different magnetic susceptibilities have been shown to form a large variety of complex structures in external magnetic fields [25].

In highly asymmetric bidisperse systems of spheres with induced dipolar interactions, clustering leads to ring-like and flame-like clusters of small spheres around strings of large spheres. Mixtures of more similarly sized particles can form strings containing both types of spheres, sometimes regularly ordered. As the interactions causing these structures are induced by an external field, this provides a way of obtaining a variety of structures from spherical colloidal particles. A wider range of cluster shapes opens up if dipolar hard dumbbells are considered, with two spheres fused at a fixed distance. By tuning the size ratio and the ratio of dipole moments between the two parts of the dumbbell, a wide variety of structures can be formed. In earlier studies, in which magnetic particles and fields were used, various chiral structures were observed in similar systems, both experimentally [26] and in simulations [27].

In preliminary experiments using our methodology based on electric fields presented in [17], but with mixtures of beads of different size and dumbbell shaped particles, we observed that the range of possible structures and parameters is enormous. We decided therefore, based on the preliminary experiments (some of which are shown in this paper), to further investigate the dipolar mixtures and dumbbells with computer simulations.

In particular, we study the formation of ringed and alternating strings in binary mixtures of spheres, and the structure of strings formed in systems consisting of asymmetric dumbbells. In the case of binary systems, the field strengths needed to form binary strings are often so high that the string fluid phase is metastable with respect to a broad phase coexistence between a dilute gas phase and a crystalline phase. However, due to the lower mobility of the larger strings compared to the single particles, the system can get kinetically trapped into a metastable fluid for long times at low packing fractions. As a result, one can study the resulting strings out of equilibrium in both experiments and simulations. As mentioned, we compare our results with preliminary experimental observations; the experimental procedure is outlined in the appendix.

The remainder of this paper is structured as follows. In section 2, we describe the models and simulation methods

used in this work. Section 3 describes the self-assembled structures observed in binary mixtures of spheres with induced dipolar interactions, including ringed and alternating strings. In section 4 we investigate the structures formed by asymmetric dipoles in external fields. Finally, we outline in section 5 how the string length distribution in monodisperse systems can be predicted theoretically, a result which can be useful to experimentally determine the particle polarizability.

2. Model and simulation methods

We examine both hard and charged colloids in an electric field. For homogeneous particles of the same material, the dipole moment in an external field is proportional to its volume, leading to stronger dipole moments for larger particles. We model the dipolar interactions as those between point dipoles in the center of the spheres. This approximation results in slightly weaker attractions at short interparticle separations compared to more detailed calculations of the polarization of spherical particles [33, 28]. However, apart from a shift in effective field strength, we expect the effects of the point-dipole approximation on the phase behavior to be minimal. The dipole–dipole interaction for two particles with diameters σ_i and σ_j is given by

$$\beta u_{\text{dip}}(r_{ij}, \theta_{ij}) = \frac{\gamma_{ij}}{2} \left(\frac{\sigma}{r_{ij}} \right)^3 (1 - 3 \cos^2 \theta_{ij}) \quad (1)$$

where $r_{ij} = |\mathbf{r}_i - \mathbf{r}_j|$ is the center-of-mass distance vector between particles i and j , θ_{ij} the angle of \mathbf{r}_{ij} with the dipole moment (oriented along the direction of the external electric field), $\beta = 1/k_B T$ with k_B is Boltzmann's constant and T the temperature. We use the particle diameter σ as unit of length, which is chosen to be the diameter of the largest particle in the case of a binary mixture.

The factor γ_{ij} is determined by the strength of the electric field, which is chosen to be uniform along the z -axis:

$$\gamma_{ij} = \frac{\pi \sigma_i^3 \sigma_j^3 \alpha^2 \epsilon_s |\mathbf{E}_{\text{loc}}|^2}{8 k_B T \sigma^3}. \quad (2)$$

Here, $\alpha = (\epsilon_p - \epsilon_s)/(\epsilon_p + 2\epsilon_s)$ is the polarizability of the particles, ϵ_s is the dielectric constant of the solvent, ϵ_p is the dielectric constant of the particle, and \mathbf{E}_{loc} is the local electric field. We define γ as the value of γ_{ij} for two particles of the largest size present in the system. We are aware of the fact that in general the polarizability should be described with a frequency dependent complex number, but we limit ourselves here to the case where only the particle dielectric contrast plays a role. In the experiments we have chosen a frequency so high (1 MHz) that the ions cannot follow the field.

The hard-sphere interaction is given by

$$\beta u_{\text{hs}}(r_{ij}) = \begin{cases} 0, & r_{ij} \geq \sigma_{ij} \\ \infty, & r_{ij} < \sigma_{ij}, \end{cases} \quad (3)$$

with $\sigma_{ij} = (\sigma_i + \sigma_j)/2$. In the case of charged spheres, a Yukawa potential is used to model the charge repulsions. For the interaction between particles of different sizes, we assume

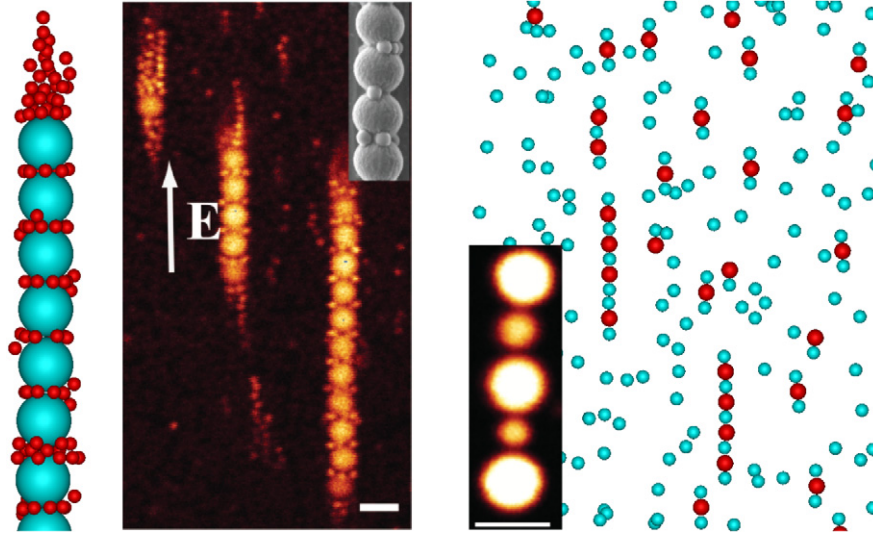


Figure 1. Left: part of a snapshot of a typical configuration of a string of 15 large particles with rings of small particles, at the size ratio $q = \sigma_S/\sigma_L = 0.25$ and $\gamma = 300$. The field is along the vertical axis, and surrounding small particles have been removed. Middle: a confocal image and a scanning electron microscopy picture of an experimental system of strings with ring-like and flame-like clusters. The particles in the experiments are poly-(methylmethacrylate) (PMMA) spheres with diameters $\sigma_L = 2.4 \mu\text{m}$ and $\sigma_S = 0.6 \mu\text{m}$. The scale bar is $2 \mu\text{m}$. Right: typical snapshot of a bidisperse system of dipolar hard spheres at size ratio $\sigma_S/\sigma_L = 0.8$, with $N_S/N_L = 10$. Here, $\gamma = 102$, $\kappa\sigma_S = 1.0$, and $Z_S^2\lambda_B/\sigma_S = 100$. Most of the gaps between two large spheres contain exactly one small sphere. The field is along the vertical axis. The picture at the bottom left is a confocal image of a binary system of PMMA spheres with diameters $\sigma_L = 1.5 \mu\text{m}$ and $\sigma_S = 1.05 \mu\text{m}$.

that the pair potential is given by the linear superposition approximation of the DLVO theory [29, 30]:

$$\beta u_Y(r_{ij}) = \begin{cases} \epsilon_{ij} \frac{\exp(-\kappa(r_{ij} - \sigma_{ij}))}{r_{ij}/\sigma}, & r_{ij} \geq \sigma_{ij} \\ \infty, & r_{ij} < \sigma_{ij} \end{cases} \quad (4)$$

$$\epsilon_{ij} = \frac{Z_i Z_j}{(1 + \kappa\sigma_i/2)(1 + \kappa\sigma_j/2)} \frac{\lambda_B}{\sigma} \quad (5)$$

where Z_i is the charge of particle i , κ^{-1} is the Debye screening length, and $\lambda_B = e^2/4\pi\epsilon_0\epsilon_s k_B T$ is the Bjerrum length with e the elementary charge and ϵ_0 the vacuum permittivity.

We performed Monte Carlo (MC) simulations in the NVT ensemble, i.e. we fixed the number of particles N , the volume V and the temperature T of the system. To handle the long-range dipolar interactions, we use Ewald summations with conducting boundary conditions [31, 32]. To improve equilibration and sampling speed in systems with strings, cluster moves were introduced to move particles residing in a cylindrical volume collectively. To maintain detailed balance, cluster moves that would change the number of particles present in this cylindrical volume were rejected.

Additionally, we perform simulations of hard dumbbells, which we model as two fused hard spheres interacting with the pair potential (1). Rotation moves were implemented to change the orientation of the dumbbells.

3. Bidisperse systems

3.1. Flame-like and ring-like clusters of small spheres

We consider binary systems of large and small colloidal spheres with diameters σ_L and σ_S , respectively, with a large

size asymmetry. The dipolar interactions as given by (1) and (2) are much stronger between the large particles than between the small particles. As a result, the formation of strings will be dominated by the clustering of the large particles. Additionally, the small particles may aggregate with the chains formed by the large particles. Due to the interactions between small and large particles, a circular attractive potential well arises for the small particles around the contact point of two large particles in the chain, and consequently the small particles can get trapped into this well [19]. Figure 1 shows a typical snapshot of the strings formed in a Monte Carlo simulation, as well as a confocal snapshot and a scanning electron microscopy picture of similar clusters in an experimental setup, all at size ratio $q = \sigma_S/\sigma_L = 0.25$. For details on the experimental setup, see the appendix.

At a size ratio $q = 0.25$, a maximum of 14 small particles can fit geometrically in this circular well in such a way that each small particle is in contact with both large spheres. At $q = 0.33$, only up to 10 particles fit in this well. However, the repulsive interactions between the small particles reduce the number of small particles per ring in the lowest-energy state. We calculate the potential energy due to the dipolar interactions as a function of the number of small particles in the circular well around the contact point between two large spheres in a string of 2 and 15 large spheres. We plot the results for $q = 0.25$ (top panel) and 0.33 (bottom panel) in figure 2. We clearly observe that for both size ratios the number of small particles in the lowest potential energy configuration increases for longer string lengths due to a stronger attractive potential around the contact points in a string. We would like to mention here that entropic effects favor a lower number of particles per ring, as this allows

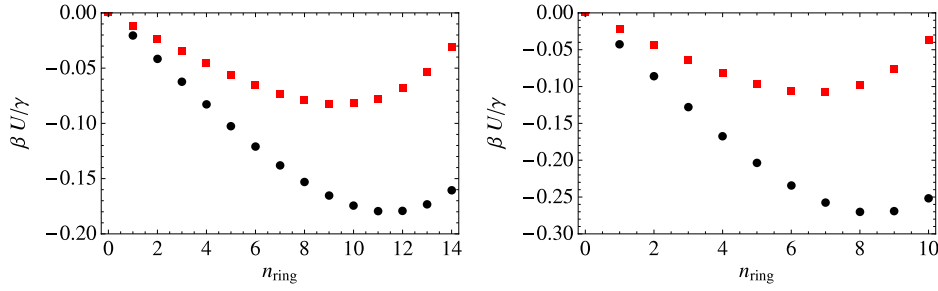


Figure 2. Potential energy of ring-like clusters of small dipolar hard spheres adsorbed near the contact point of two large dipolar hard spheres, in a string consisting of two large spheres (■) and 15 large spheres (●), as a function of the number of small spheres in the ring, i.e. n_{ring} . The size ratio between small and large spheres is $q = \sigma_S/\sigma_L = 0.25$ (left) and $q = 0.33$ (right). Interactions between the large particles are not included in the potential energy.

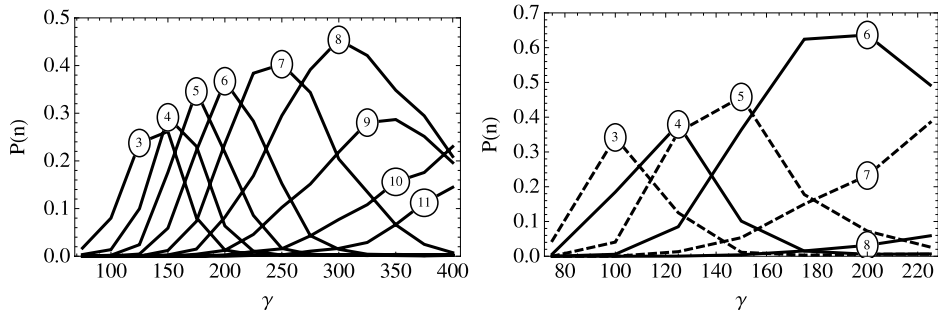


Figure 3. Probability distribution function $P(n)$ for a ring-like cluster of n small dipolar particles as a function of the field strength γ for a string of 15 large dipolar spheres, at small particle density $\eta_S = 1.9 \times 10^{-3}$. The size ratios are $q = 0.25$ (left) and $q = 0.33$ (right). The labels denote the number of small spheres n in the ring.

for more free volume or entropy both inside and outside the cluster. In addition, we find from figure 2 that for a size ratio $q = 0.25$ the small particles get trapped in this well for $\gamma \simeq 50$ as the potential energy is $\sim 0.02 k_B T$ per particle for string length 15. For such high fields, the string fluid of large particles is thermodynamically metastable with respect to a broad gas–solid transition [6]. In experiments, the large strings are partially stabilized by inhomogeneities in the external field, causing the strings to stay in local areas of high field strength and preventing them from clustering together. In standard MC simulations (without any (unphysical) cluster moves), the clustering of strings is inhibited as the mobility of the self-assembled strings is extremely low. Since the interactions with the small particles are much weaker, the small spheres can still sample phase space, and can reach equilibrium within the constraints given by the configuration of the larger particles.

Due to the dipolar interactions between the small and large spheres, the small spheres can also aggregate in a large potential well at the end of the chains (see the left side of figure 1). The resulting aggregate of small particles is wider near the string of large particles. In addition, the fluctuations of the cluster are more pronounced far from the strings, giving a flame-like shape to the cluster. Due to the larger and deeper potential well, a flame-like cluster will generally contain more small spheres than a ring-like cluster, in good correspondence with what was observed in the experiments.

In order to study the structure of the binary strings, we performed MC simulations to study binary strings of dipolar

hard spheres with a size ratio $q = 0.25$ and 0.33 , both starting from a homogeneous random initial configuration, and from a configuration containing a single string of large spheres in a sea of small spheres. For the simulations starting from a random configuration, we used 100 large particles, and varied the number of small particles from 100 to 600. The overall packing fraction was well below 1% ($\eta_L = 0.002$), to keep the strings of large spheres from clustering. We indeed observe that the large particles self-assemble in linear strings parallel to the field direction and that small particles form ring-like and flame-like clusters around the strings of larger spheres. To determine the probability distribution of the number of small spheres in the ring-like clusters, we perform Monte Carlo simulations of a string of 15 large spheres at varying densities of small spheres. While the large spheres were allowed to move in the simulation, field strengths were always sufficiently high to prevent the string from breaking.

At the field strengths where the ring-like clusters are regularly seen, the flame-like clusters always appear as well. The presence of small particles near the ends of the strings of large spheres hinders the formation of long strings in the simulation, as it can take a long time ($\gtrsim 10^5$ MC cycles) for the small particles to be pushed away from two merging strings. The ring-like clusters can be seen in a wide range of field strengths, and the occupancy of the ring rises as γ increases. Figure 3 shows the probability distribution functions $P(n)$ of observing n small spheres in a ring as a function of field strength γ as determined from simulations, for size ratios of 0.25 and 0.33 . The plots show a continuous increase in the

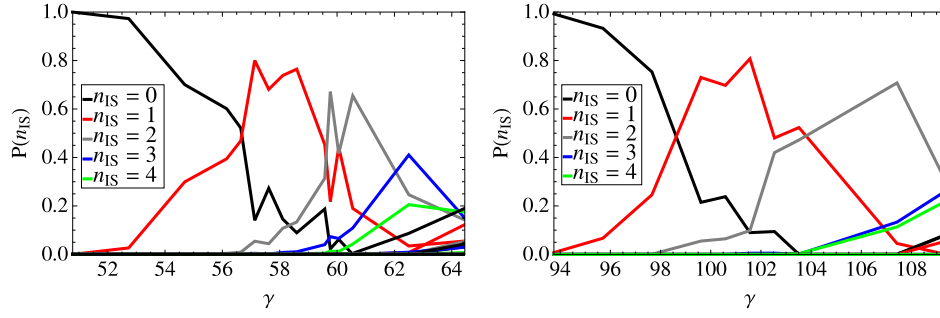


Figure 4. Probability distribution function $P(n_{IS})$ of the number n_{IS} of interstitial small dipolar particles between a pair of large dipolar spheres in a string, for $\kappa\sigma_S = 1.00$, $\eta_L = 6.3 \times 10^{-4}$, and $\eta_S = 2.9 \times 10^{-3}$, as a function of the field strength γ . The size ratio is $\sigma_S/\sigma_L = 0.8$. The particle charges for the left and right plot are given by $Z_S^2\lambda_B/\sigma_S = 50$ and 100, respectively.

number of small spheres per ring as a function of γ , as well as a preference over a large range of field strengths for eight particles per ring at a size ratio of 0.25 and six at a size ratio of 0.33. It should be noted that the total number of small particles in the system is constant, and trapping many small particles in the ring-like and flame-like clusters decreases the density of free small particles. However, changing the density of small spheres did not change the probability distribution functions significantly.

For very high field strengths, we observe the formation of thicker ring-like clusters of small spheres around the contact point between two large spheres. Due to the weaker potential wells further away from the string, these thicker rings tend to be more disordered, and exchange small particles with the surrounding fluid at a faster rate.

3.2. Alternating strings

For less asymmetric systems, we observe the formation of binary strings that consist of alternating large and small particles. We are specifically interested in finding out if it is possible to find a region in parameter space where almost all (metastable) strings formed consist of regular large–small sequences. To investigate this, we studied the self-assembly of these strings for both hard and charged dipolar particles, using MC simulations of systems with several size ratios and a range of stoichiometries. The electrostatic repulsions are described by screened-Coulomb interactions (see (4)), where the charge Z is chosen to be proportional to the surface area of the spheres. In all cases, the total packing fraction was below 1%. The simulations were performed in a rectangular box, elongated along the z -axis to allow for longer strings. All simulations are started from a random initial configuration. On the right in figure 1 we show a typical snapshot of the strings formed in a system of charged particles, together with a confocal image of a short alternating string taken from experiments.

The formation of alternating strings can be understood by the bond between a large and a small particle being significantly stronger than the bond between two small particles. In systems with many more small dipolar particles than large particles, the large particles will first bond with a small number of small ones on each side shortly after the

field is turned on. These clusters will then join to form longer strings, with several interstitial small particles between the large ones. While in equilibrium the large particles are bonded in a string, the removal of the small particles is a slow process. The free energy barrier that these small particles have to overcome to escape the string is dependent on the number of small particles between two large spheres, and is highest for one small particle with two large neighbors.

For uncharged dipolar spheres, alternating strings were not observed with any regularity, as the potential energy differences are too small between configurations with one, two, or three small spheres in between two large ones. As a result, in sufficiently long simulations all interstitial small particles are removed from the strings, resulting in strings of large particles only with small particles exclusively at the ends.

Interestingly, simulations of charged particles show the self-assembly of alternating strings that remain stable on much longer timescales. Since the charge on each particle scales with the surface area, the bonds between the large spheres are relatively weaker, and hence configurations with more than one small particle between two large spheres in a string become less stable. While defects always appear, for inverse screening lengths of the order of σ_S and a size ratio of $\sigma_S/\sigma_L = 0.8$, the average number of small particles between two large spheres in a string can be tuned by the field strength. In order to study the field-strength dependence of the number of interstitial small spheres n_{IS} in between a pair of large spheres in a string, we determine the probability distribution function $P(n_{IS})$ for varying γ .

Figure 4 shows the distribution of a number of small colloids between two large ones in the strings, for two different numbers of charges per colloid. The simulations consisted of $N_L = 50$ large and $N_S = 500$ small particles, at an overall packing fraction of 3.5×10^{-3} . Increasing the field strength increases the number of small particles per gap, as the stronger attractions hinder the escape of small particles from the strings. Interestingly, a large fraction of trimers, with one large particle sandwiched by two small particles, is also often seen in addition to the longer strings. While forming alternating strings is much easier with an added Yukawa repulsion, the formed configurations are still metastable states: if swap moves are introduced into the

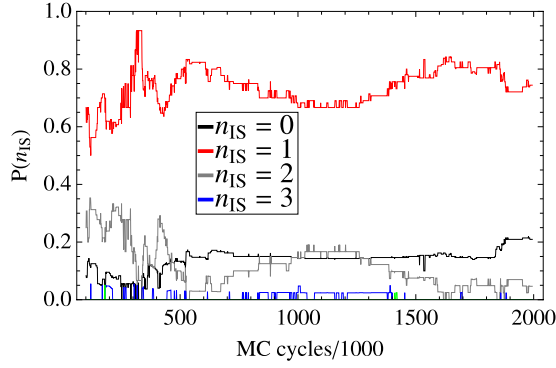


Figure 5. Time dependence of the probability distributions $P(n_{IS})$ shown in figure 4, showing how n_{IS} changes as a function of the number of MC cycles, where one MC cycle consists of $N_S + N_L$ trial moves of the particles. The same parameters were used as in figure 4, with $Z_S^2 \lambda_B / \sigma_S = 50$ and $\gamma = 58.6$.

simulations, allowing a large and small particle to switch positions, the alternating strings rapidly change into strings consisting mainly of large spheres. However, without swap moves, these structures are stable even in long simulations, and the distribution of the number of small particles between two larger ones is approximately constant after equilibration, as shown in figure 5 and as seen in preliminary experiments.

4. Asymmetric dumbbells

Finally, we investigate strings in a system of asymmetric hard dumbbells in an external electric field. Each dumbbell particle consists of a large and a small sphere, with diameters σ_L and σ_S , respectively, and a fixed separation distance $d \leq \sigma_{LS}$, where $\sigma_{LS} = (\sigma_L + \sigma_S)/2$. In general, determining the interactions of polarized anisotropic particles is a complex task [33]. Here, we approximate the interaction between the spheres by the interaction between point dipoles at the sphere centers, which interacts with all others via the potential

$$\beta u_{\text{dip}}(r_{ij}, \theta_{ij}) = \frac{\gamma p_i p_j}{2p_L^2} \left(\frac{\sigma}{r_{ij}} \right)^3 (1 - 3\cos^2 \theta_{ij}). \quad (6)$$

Here, the dipole strength p_i for sphere i is determined by the size of the sphere, and is equal to either p_L or p_S for large and small spheres, respectively. The relative interaction strengths for the two types of spheres is therefore controlled by the ratio p_S/p_L , while the absolute interaction strength is determined by $\gamma = \gamma_{LL}$, as defined in (2).

Due to the interaction between the two spheres in a single dumbbell, a single particle favors an orientation aligned along the direction of the field. Magnetic colloidal particles of this type have been seen to form chiral structures in experimental systems where the smaller part of the dumbbell acquires a much stronger dipole moment in the external magnetic field [26]. Recently, a variety of helical structures has been characterized as global potential minima for clusters of asymmetric dumbbells consisting of two Lennard-Jones particles and a point dipole directed across the axis between the spheres [27]. Chiral structures have also been predicted to

occur in systems of dipolar hard spheres in the presence of depletion interactions [34]. Finally, confinement of (hard or charged) spherical particles in cylindrical geometries has been shown to lead to chirality, depending on the ratio between the sphere and cylinder diameters [35–37, 34].

Similar to systems of dipolar spheres, asymmetric dipolar dumbbells form strings at low field strengths and packing fractions, which grow in length and thickness as γ increases. We investigate the zero-temperature structure of these strings, and perform Monte Carlo simulations to study the behavior at finite temperatures.

We first consider hard dumbbells consisting of two adjacent hard spheres at separation distance $d = \sigma_{LS}$. The structure of a single string in the limit of strong fields (or zero temperature) mainly depends on the size ratio of the dumbbell σ_S/σ_L and the ratio between the dipole moments of the two spheres p_S/p_L . By comparing the potential energy for a number of possible configurations, we can draw a phase diagram of the predicted structures as shown in figure 6. The candidate structures considered were head-to-toe and head-to-head strings, buckled strings, columnar structures, and helical structures. In the head-to-toe or head-to-head configuration, all spheres are centered on a straight line, with all the dumbbells oriented in the same direction or alternating between ‘up’ and ‘down’, respectively. The buckled strings consist of a central string of large spheres, with the smaller spheres pushed to either the side or the end of the string. When the dipole moment of the smaller spheres is sufficiently large, the central string consists of smaller spheres instead. For the size ratio $\sigma_S/\sigma_L > 0.5$, the larger spheres arrange into two adjacent columns. For $\sigma_S/\sigma_L < 0.5$, the structure formed can either consist of two sets of these columns, or helical structures, strongly depending on the size ratio.

If the dipole moment of the spheres scales with the volume of the spheres, as would be the case if both parts are made out of the same material, the large particles will have the stronger dipole moment. The dashed line in figure 6 shows the structures formed in this case. Depending on the size ratio, the string only takes two shapes: aligned dumbbells in head-to-head orientations, or a string of large particles with the small particles all on the same side (except at the ends).

We wish to remark here that it is possible that we missed some structures, which can change the phase diagram. In particular, for highly asymmetric dumbbells where the dipole moment of the small sphere is large, the potential energies of helical and columnar structures are close together. Since we only calculated the potential energies of a limited set of candidate cluster configurations, with highly regular orientations of the particles within the string, the possibility of more irregular structures being favored cannot be discounted. Therefore, the phase diagram shown in figure 6 is mainly a qualitative indication of the expected cluster shapes. However, the structures in the ground-state phase diagram agree qualitatively with structures seen in simulations using high field strengths.

The boundaries between the different structures shift slightly based on the length of the string, but the observed structures remain the same for longer strings. While changing

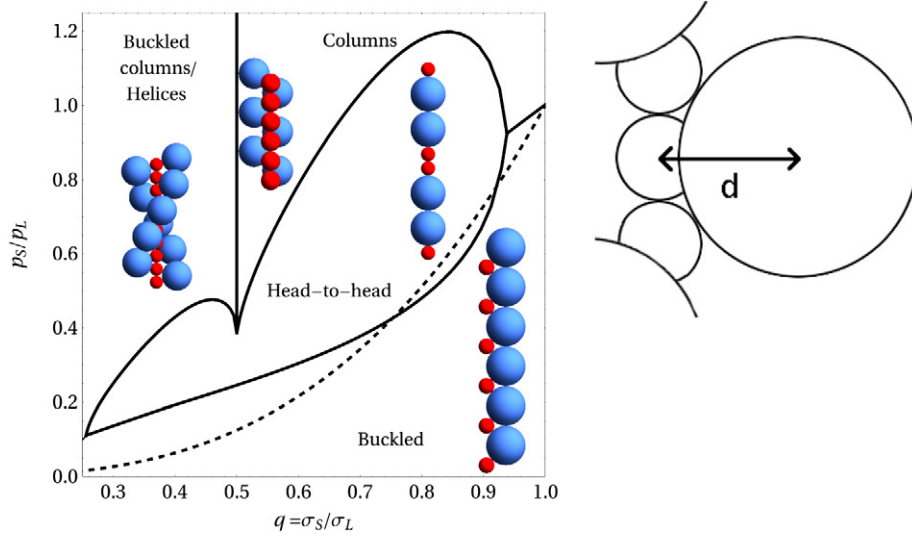


Figure 6. Left: ground-state phase diagram for strings of 15 asymmetric dumbbells, as a function of size ratio q and dipole moment ratio p_s/p_L . The head-to-head configurations consist of alternating pairs of large and small spheres, while the buckled strings are strings of large particles with the small ones positioned at the contact points of two large particles. The columnar or helical structures consist of strings of small spheres with the large spheres arranged in multiple columns or in a helical structure. The dashed line illustrates dumbbells made out of one material. Right: cartoon of three dumbbell particles arranged in a string, with d chosen such that the large part of the middle dumbbell touches the two small parts of its neighbors, i.e. $d = d_t$.

the center-of-mass distance d has some influence on the boundaries of these regimes, it does not seem to qualitatively change most of the self-assembled structures. However, changing d can strongly influence the columns and helices found at low size ratios with $p_L < p_s$.

To further investigate the possibility of helical strings, we performed simulations of highly asymmetric dumbbells, where the dipole moment of the small spheres was much larger than that of the large spheres. For sufficiently high field strengths, the small spheres will form a string, with the large spheres sticking out to the sides. Depending on the size ratio, these large spheres can form either columns around the central string, or helical structures. These chiral structures appear due to the frustrations caused by hard-core interactions between the large spheres, which prevent them from lining up along the field direction. By constraining the large spheres to a narrow ring-like volume around their smaller partners, these frustrations cannot be compensated by small deviations parallel to the string. This restriction can be obtained by choosing the distance d between the two spheres of a dumbbell close to the minimum value d_t where the large particles touch the small spheres of nearby dumbbells in the string, as shown on the right in figure 6. For this case, the ground-state structures we obtained are shown on the left side of figure 7 for six different size ratios.

From the potential energy minimization, we find that at size ratios just above $\sigma_L/\sigma_s = 0.5$ the large spheres form two columns close together and aligned parallel to the string. At slightly larger size ratios, this configuration would lead to overlaps, and each column becomes buckled. In this case, the two buckled columns tend to be on opposite sides of the string. For the size ratio $q < 0.47$, the structure changes from columns to a double helix, decreasing in pitch length as q decreases. Close to a size ratio of $q = 0.33$, the structure

crosses over to three vertical columns, turning into a triple helix once $q < 1/3$. For size ratios $q < 0.28$, the large spheres will overlap in any configuration. At this point, the string of small particles will always be deformed.

We now perform MC simulations to investigate the formation of these structures. To this end, we first carried out a normal simulation at low field strength ($\gamma_{SS} \simeq 20$), to allow the dumbbell particles to form strings of sufficient length. Subsequently, we quenched these strings to high field strengths, which should then mostly affect the positions of the large spheres along these strings. These simulations were performed at low packing fractions $\eta \simeq 0.01$, with $N = 200$ dumbbell particles in the simulation box. For each size ratio, the distance d between spheres was chosen just above d_t to minimize fluctuations of the large spheres parallel to the string. Due to the high field strengths, the formation of the strings is a process far out of equilibrium. The resulting string length distribution is therefore not an equilibrium quantity that can be reliably measured from these simulations. Since we are mostly interested in the configurations of individual strings after quenching, these simulations can also be started from an initial configuration containing one long string. When quenching the system, the field strength is increased in small steps ($\Delta\gamma \simeq 1$) during the simulation, eventually freezing the system into a local energy minimum. At this point, we observe the resulting structures. Long strings form readily in systems with $q > 0.4$. For $q < 0.4$, the hard cores of the large spheres hamper the formation of strings of more than four or five dumbbells. More asymmetric size ratios will also hinder reconfigurations within the string, as the hard-core interactions severely limit the rotational freedom of the dumbbells. While chiral structures can be found in these simulations, defects and changes in the handedness are regularly seen, since both directions of chirality have equal probability.

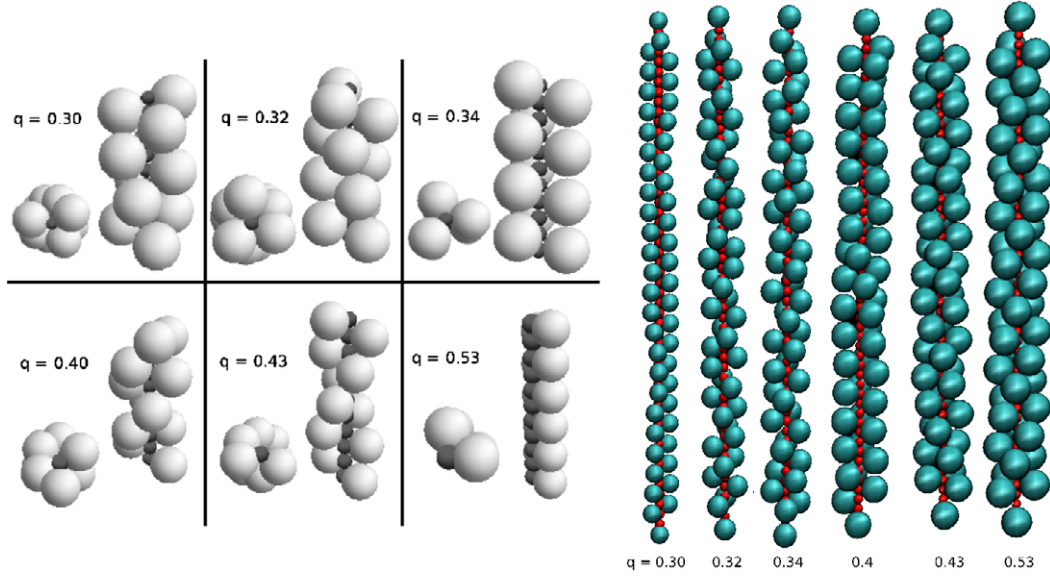


Figure 7. Left: structures resulting from the minimum energy calculations, at various size ratios. Here, $d = d_t + 0.01\sigma_L$, the same values as used in the simulations. The numbers indicate the size ratio q . Both a side view and a top view are shown for each size ratio. Right: strings of dipolar asymmetric dumbbells resulting from simulations starting with a string consisting of 50 particles, quenched to high field strengths, at various size ratios q as labeled and center-of-mass distance $d = d_t + 0.01\sigma_L$.

On the right side of figure 7, we show snapshots from simulations starting from an initial configuration consisting of a straight string of 50 randomly oriented dumbbells. After quenching, we observe that structures are formed similar to the predicted ground-state structures, although defects in the structures exist in the structures resulting from simulations, as the system can get trapped in local energy minima during the quench. In these simulations, the dipole moment of the small spheres is five times that of the large spheres, which is large enough to prevent breaking or bending of the string. While the simulated strings show good agreement with the ground-state structures shown in figure 7, the spontaneous formation of regular chiral structures appears to be difficult. This may be a severe problem for experimentalists attempting to fabricate helical strings of asymmetric dumbbells by applying an external electric field. The difficulty can be explained by the fact that the energy costs involved in defects (which depend largely on next-nearest neighbor interactions) are small compared to the gain in entropy for additional disorder in the string. Additionally, the free energy barrier that has to be overcome to change the local direction of the chirality in a string is large, due to both hard-core interactions and attractive forces.

5. Equilibrium string length distribution in monodisperse systems

In addition to the more complex systems discussed in this paper, we investigated the string fluid regime for monodisperse dipolar hard spheres using *NVT* MC simulations of $N = 1200$ particles with diameter σ in a simulation box elongated along the field direction in order to accommodate long strings. We measured the probability distribution function $P(n)$ of string length n in the system for

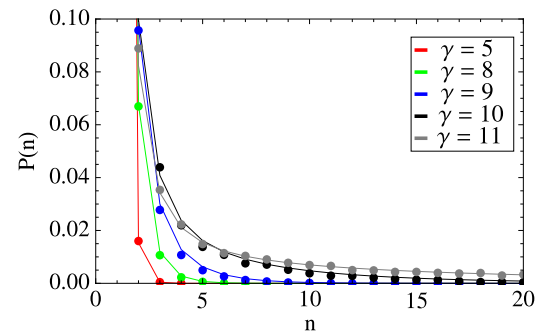


Figure 8. String length distribution $P(n)$ with n the number of spheres in a string for a fluid of dipolar hard spheres at packing fraction $\eta = 7.1 \times 10^{-4}$ and for various field strength γ as labeled. The symbols are obtained from simulations and the lines show the predictions from Wertheim theory.

varying field strength γ . In figure 8 we plot $P(n)$ as a function of the number of particles n in a string for $\gamma = 5, 8, 9, 10$, and 11 , at a constant packing fraction $\eta = \pi\sigma^3 N/6V = 7.1 \times 10^{-4}$. The simulation results are denoted by the symbols. As expected, the average length of the strings increase with both dipole strength γ and packing fraction η . When the field strength is larger than $\gamma \simeq 10$, strings start spanning the simulation box, and simulation results become unreliable. Additionally, sufficiently long strings attract each other and can cluster into thicker strings at high field strengths [40]. Here, we will investigate the string length distribution in the regime where the strings are clearly separated, ensuring a well-defined string length.

We compare our results with the first-order thermodynamic perturbation theory of Wertheim, which yields free energy predictions for associating fluids [41–43]. These free energy expressions can be used to predict the distribution of cluster sizes in equilibrium systems [44]. While the theory

is more suitable for particles with short-ranged interactions, it can be adapted to quantitatively describe the formation of strings in a dipolar system.

To this end, we consider colloidal spheres with two binding sites in diametrically opposite positions. The first-order thermodynamic perturbation theory of Wertheim is based on the assumption that each binding site can only form one bond with another particle and that pairs of particles can only be single bonded. These assumptions are satisfied in the string fluid regime for monodisperse dipolar spheres, assuming the packing fraction and field strength are low enough to ensure that all strings are well separated. In this case, each particle can form a bond with at most two other particles. According to Wertheim theory the probability p_b that an arbitrary binding site is bonded can be determined from the chemical equilibrium between two non-bonded particles and a dimer cluster:

$$\frac{p_b}{(1-p_b)^2} = \rho \Delta, \quad (7)$$

where Δ is calculated by integrating the Mayer function $f(\mathbf{r}) = \exp(-\beta u_{\text{dip}}(\mathbf{r})) - 1$ over the volume of a binding site [41–43]:

$$\Delta = \int_{\text{site}} d\mathbf{r} g(\mathbf{r}) f(\mathbf{r}) \quad (8)$$

$$\simeq 2\pi \int_{\theta=0}^{\theta_{\max}} d\theta \int_{r=\sigma}^{r_{\max}} dr f(r, \theta) r^2 \sin \theta, \quad (9)$$

with $g(r)$ the pair correlation function of a reference system at the same packing fraction. As the packing fractions for the studied string fluid systems are low, we use the ideal gas approximation $g(\mathbf{r}) \simeq 1$.

As the integral in (9) is over the volume of a single bonding site, θ_{\max} is chosen to be the edge of this bonding site, where $u_{\text{dip}}(r, \theta) = 0$. The integral diverges logarithmically for $r \rightarrow \infty$, and therefore we have to choose a reasonable limit r_{\max} for the distance at which particles can still be considered bonded. We have set $r_{\max} = 2\sigma$.

In addition, the number density of monomers is $\rho_1 = \rho(1-p_b)^2$, since for a monomer both sides are unbonded. Here we define $\rho = N/V$ as the particle number density. Similarly, the number density ρ_n of strings of length n is

$$\rho_n = \rho(1-p_b)^2 p_b^{n-1}, \quad (10)$$

as the first and last particle in the chain have one unbonded site each. From (7), we can easily determine p_b once Δ is known. Using the bond probability p_b , we can determine the cluster size distribution $P(n)$:

$$P(n) = \frac{\rho_n}{\sum_{i=1}^{\infty} \rho_i} = (1-p_b) p_b^{n-1}, \quad (11)$$

where $P(n)$ is the probability that a randomly selected string has a length of n , and $\sum_{i=1}^{\infty} \rho_i = \rho(1-p_b)$, obtained by summing the geometric series over all chain lengths.

However, in our system there are correlations between nearby bonds, since the attractive potential of the dipoles extends beyond the distance of a single particle. As a result, a

particle is more likely to be attached to longer strings. If we assume that neighboring particles in the string are at contact along the z -axis then the potential near the top of a string of length n is given by:

$$u(\mathbf{r}, n) = \sum_{i=0}^{n-1} u_{\text{dip}}(\mathbf{r} - i\hat{\mathbf{z}}). \quad (12)$$

This potential can then be used to calculate $\Delta(n)$ using (9) with the Mayer function corresponding to $u_n(\mathbf{r}, n)$. Subsequently, we can write a recursive relation for ρ_n :

$$\frac{\rho_n}{\rho_{n-1}\rho_1} = \Delta(n). \quad (13)$$

To calculate ρ_1 , we normalize this distribution using

$$\sum_{n=1}^{\infty} n \rho_n = \rho. \quad (14)$$

We plot the theoretical results (solid lines) along with the simulation results in figure 8. The theoretical predictions fit the simulation data for low packing fractions and field strengths very well, as shown in figure 8. We obtain agreement between theory and simulations as long as the simulated strings do not cluster together or span the simulation box. As no fit parameters are required in the theory to match the simulation data, Wertheim theory allows a direct quantitative prediction of the distribution of string lengths in the dilute string fluid regime of hard dipolar spheres. In principle, it should also be straightforward to extend this theory to charged dipolar spheres, by adding a Yukawa repulsion in (9). Using these theoretical predictions for the cluster size distribution, an estimate for the effective field strength γ could be obtained from experimentally measured string length distributions.

6. Conclusions

We investigated the self-assembly and structure of strings in systems of colloidal particles with dipole moments induced by an external field. In binary systems, strings of large particles with both ring-like and flame-like clusters of small particles can be formed in highly asymmetric systems, where $q = \sigma_S/\sigma_L \ll 1$. In systems with a size ratio of $q = 0.8$ alternating strings can be formed instead. While these structures are not thermodynamically stable, they persist in simulations on very long timescales, and have been observed in experiments as well.

Additionally, we studied the strings formed by asymmetric hard dumbbells in the presence of a strong electric field. When the particles are made out of a single material, the lowest-energy structures are head-to-head strings for nearly symmetric dumbbells, and buckled strings for more asymmetric particles. However, in the case where the dipole moment of the small spheres is sufficiently high, the lowest-energy structure consists of a string of small spheres, with the large spheres either positioned in multiple columns or in a helical structure around the string. It should be noted that defects are expected to be common in spontaneously formed clusters of dumbbells, due to the large free energy barriers involved in changing the chirality of the helical structure.

Finally, we used thermodynamic perturbation theory to show how the field strength can be related to the string length distribution in monodisperse systems. Comparisons of these calculated cluster size distributions to experimentally measured ones would provide a direct way to experimentally determine the polarizability of the particles used at the applied frequency.

Acknowledgments

We acknowledge support from an NWO-VICI grant, and this work is part of the research programme of the Foundation for Fundamental Research on Matter (FOM), which is part of the Netherlands Organisation for Scientific Research (NWO). Additionally, this study is part of the FOM/DFG collaborative Transregio Network 6 on Colloids in External fields.

Appendix. Experimental setup

In the experiments shown in figure 1, the colloidal dispersion consisted of equal amounts (1.8 wt%) of small and large PMMA spheres in cyclohexyl bromide. The PMMA particles were synthesized by dispersion polymerization, covalently labeled with the fluorescent dye 7-nitrobenzo-2-oxa-1,3-diazole (NBD) or rhodamine isothiocyanate (RITC) and sterically stabilized with poly(12-hydroxystearic acid) [38]. We used both suspensions with a size ratio of 0.25 ($\sigma_L = 2.40 \mu\text{m}$ and $\sigma_S = 0.60 \mu\text{m}$) and those with a size ratio 0.7 ($\sigma_L = 1.50 \mu\text{m}$ and $\sigma_S = 1.05 \mu\text{m}$). The particles were dispersed in a 3:1 wt/wt mixture of cyclohexyl bromide (Fluka) and *cis*-decalin (Sigma), saturated with tetrabutylammonium bromide (TBAB; Sigma). In this mixture, the particles were nearly density and refractive-index-matched, and the double layer was not larger than the particle size [4]. All solvents were used as-received without any further purification. The solutions were placed in sample cells with attached electrodes. After filling the cell with the colloidal suspension, we sealed it at both ends with UV-curing optical adhesive (Norland no. 68), and we studied particle dynamics by means of confocal laser scanning microscopy (Leica TCS SP2). An oscillating electric field was applied using a function generator (Agilent, model 3312 OA) and a wide band voltage amplifier (Krohn-Hite, model 7602M). The root-mean-square of the electric field strength used was $E_{\text{rms}} = 0.45 \text{ V } \mu\text{m}^{-1}$, with a frequency $f = 1 \text{ MHz}$, which we assume to be fast enough to ensure that the ions in the double layer will not be able to follow the electric field.

After 5–6 min, all the particles were assembled into complex structures in the applied field direction. The dispersion was subsequently heated to 70–75 °C, still well below the glass transition temperature ($T_g \simeq 140 \text{ °C}$ [39]) of PMMA, for 2–3 min using a stream of hot air that was much wider than the sample cell. The sample cooled down to room temperature in 5 min, still in the presence of the electric field. The field was then turned off and confocal laser scanning microscopy revealed that the particles that were in contact had bonded permanently.

References

- [1] Parthasarathy M and Klingenberg D J 1996 *Mater. Sci. Eng. R Rep.* **17** 57
- [2] Tao R 2001 *J. Phys.: Condens. Matter* **13** R979
- [3] Wen W *et al* 2005 *Nanotechnology* **16** 598
- [4] Yethiraj A and Van Blaaderen A 2003 *Nature* **421** 513
- [5] Yethiraj A, Thijssen J H J, Wouterse A and van Blaaderen A 2004 *Adv. Mater.* **16** 596
- [6] Hynninen A-P and Dijkstra M 2005 *Phys. Rev. Lett.* **94** 138303
- [7] Chen T-J, Zitter R N and Tao R 1992 *Phys. Rev. Lett.* **68** 2555
- [8] Dassanayake U, Fraden S and van Blaaderen A 2000 *J. Chem. Phys.* **112** 3851
- [9] Zerrouki D, Baudry J, Pine D and Chaikin P 2008 *Nature* **455** 380
- [10] Velev O D and Gupta S 2009 *Adv. Mater.* **21** 1897
- [11] Smoukov S K, Gangwal S, Marquez M and Velev O D 2009 *Soft Matter* **5** 1285
- [12] Reches M, Snyder P W and Whitesides G M 2009 *Proc. Natl Acad. Sci. USA* **106** 17644
- [13] Sung K E *et al* 2008 *J. Am. Chem. Soc.* **130** 1335
- [14] Biswal S L and Gast A P 2003 *Phys. Rev. E* **68** 021402
- [15] Dreyfus R *et al* 2005 *Nature* **437** 826
- [16] Furst E M, Suzuki C, Fermigier M and Gast A P 1998 *Langmuir* **14** 7334
- [17] Vutukuri H R *et al* 2012 *Angew. Chem.* *at press*
- [18] Holm C *et al* 2006 *J. Phys.: Condens. Matter* **18** 2737
- [19] Huang J P, Wang Z W and Holm C 2005 *J. Magn. Magn. Mater.* **289** 234
- [20] Klokkenburg M *et al* 2006 *Phys. Rev. Lett.* **96** 037203
- [21] Camp P J and Patey G N 2000 *Phys. Rev. E* **62** 5403
- [22] Ivanov A O and Kantorovich S S 2003 *Colloid J.* **65** 166
- [23] Wang Z and Holm C 2003 *Phys. Rev. E* **68** 041401
- [24] See H, Kawai A and Ikazaki F 2002 *Rheol. Acta* **41** 55
- [25] Erb R M *et al* 2009 *Nature* **457** 999
- [26] Zerrouki D *et al* 2008 *Nature* **455** 380
- [27] Chakrabarti D, Fejer S N and Wales D J 2009 *Proc. Natl Acad. Sci. USA* **106** 20164
- [28] Pitkonen M 2008 *J. Appl. Phys.* **103** 104910
- [29] Verwey E J W and Overbeek J T G 1948 *Theory of the Stability of Lyotropic Colloids* (Amsterdam: Elsevier)
- [30] Bell G M, Levine S and McCartney L N 1970 *J. Colloid Interface Sci.* **33** 335
- [31] Frenkel D and Smit B 2002 *Understanding Molecular Simulations: From Algorithms to Applications* (San Diego, CA: Academic)
- [32] Ewald P P 1921 *Ann. Phys.* **369** 253
- [33] Kwaadgras B W, Verdult M, Dijkstra M and van Roij R 2011 *J. Chem. Phys.* **135** 134105
- [34] Pickett G T, Gross M and Okuyama H 2000 *Phys. Rev. Lett.* **85** 3652
- [35] Oğuz E C, Messina R and Löwen H 2011 *Europhys. Lett.* **94** 28005
- [36] Mughal A, Chan H K and Weaire D 2011 *Phys. Rev. Lett.* **106** 115704
- [37] Chan H-K 2011 *Phys. Rev. E* **84** 050302
- [38] Bosma G *et al* 2002 *J. Colloid Interface Sci.* **245** 292
- [39] Vutukuri H R *et al* 2012 *Adv. Mater.* **24** 412
- [40] Satoh A, Chantrell R W, Kamiyama S-I and Coverdale G N 1996 *J. Colloid Interface Sci.* **181** 422
- [41] Wertheim M S 1984 *J. Stat. Phys.* **35** 19
- [42] Wertheim M S 1984 *J. Stat. Phys.* **35** 35
- [43] Wertheim M S 1986 *J. Stat. Phys.* **42** 459
- [44] Sciortino F, Bianchi E, Douglas J F and Tartaglia P 2007 *J. Chem. Phys.* **126** 194903